Euro. Jnl of Applied Mathematics (2002), *vol.* 13, *pp.* 1–23.
DOI: 10.1017/S0956792501004740 Printed in the United Kingdom

Deformation of nematic liquid crystals in an electric field

R. H. SELF[1], C. P. PLEASE[2] and T. J. SLUCKIN[2,3]

[1]*Institute of Sound & Vibration Research, University of Southampton, Southampton S017 1BJ, UK*
[2]*Faculty of Mathematical Studies, University of Southampton, Southampton S017 1BJ, UK*
[3]*Liquid Crystal Institute, University of Southampton, Southampton S017 1BJ, UK*

(*Received 28 November 2000; revised 13 July 2001*)

The behaviour of liquid crystal materials used in display devices is discussed. The underlying continuum theory developed by Frank, Ericksen and Leslie for describing this behaviour is reviewed. Particular attention is paid to the approximations and extensions relevant to existing device technology areas where mathematical analysis would aid device development. To illustrate some of the special behaviour of liquid crystals and in order to demonstrate the techniques employed, the specific case of a nematic liquid crystal held between two parallel electrical conductors is considered. It has long been known that there is a critical voltage below which the internal elastic strength of the liquid crystal exceeds the electric forces and hence the system remains undeformed from its base state. This bifurcation behaviour is called the Freedericksz transition. Conventional analytic analysis of this problem normally considers a magnetic, rather than electric, field or a near-transition voltage since in these cases the electromagnetic field structure decouples from the rest of the problem. Here we consider more practical situations where the electromagnetic field interacts with the liquid crystal deformation. Assuming strong anchoring at surfaces and a one dimensional deformation, three nondimensional parameters are identified. These relate to the applied voltage, the anisotropy of the electrical permittivity of the liquid crystal, and to the anisotropy of the elastic stiffness of the liquid crystal. The analysis uses asymptotic methods to determine the solution in a numerous of different regimes defined by physically relevant limiting cases of the parameters. In particular, results are presented showing the delicate balance between an anisotropic material trying to push the electric field away from regions of large deformation and the deformation trying to be maximum in regions of high electric field.

1 Introduction

Liquid crystals display a rich diversity of behaviour which is reflected by the complexity of their governing equations and the large number of material parameters involved. A general survey can be found in de Gennes & Prost [6] and more detailed accounts in the references given below. Liquid crystals are anisotropic materials whose (often elongated) molecular structure induces a locally preferred common direction, described by means of a unit vector **n**, called the director. Several types of liquid crystal exist depending on the spatial distribution of the director in the absence of distorting influences and whether or not some degree of positional order exists in addition to the orientational order. The simplest are nematics and cholesterics. In nematics there is a globally preferred direction

and, when undisturbed, **n** is constant throughout the sample, while for cholesterics the locally preferred direction varies in such a way that the director twists to form a helical pattern.

Despite the great many studies undertaken, much of the behaviour of liquid crystals is yet to be systematically investigated and this is as true of nematics and cholesterics as it is of the more complicated smectic liquid crystal phases. From a practical point of view, and in spite of interest in new electro-optic devices that use smectic materials, there is still considerable interest in novel and improved nematic devices. In addition there are a great many parallels between the behaviour of nematics and smectics which makes the systematic investigation of the simpler nematic phase an important task. Some recent results in the theory of both smectics and nematics was recently reported in a special edition of this journal [19].

From a technological point of view the main interest is in the optical properties of devices but these can only be modified by altering the director field. Consequently determining the behaviour of the director field is the crucial problem of interest. The desired improvements in optical performance of devices relating, for instance, to speed of operation, adequate grey scale, large viewing angles and stability to external disruption, can all be interpreted as requirements on the underlying director field.

The tendency of the director to take on a particular spatial distribution can be understood in terms of the elastic continuum theory first proposed by Oseen and Zöcher and popularised and developed by Frank [11]. In this theory elastic forces arising from the molecular structure of the material, resist any distortion to the director field from its equilibrium state. These distortions can arise for a number of reasons including: interaction with external fields (typically magnetic or electric), coupling with the material flow of the liquid, and from interactions with confining surfaces. When subjected to competing influences the director will adjust throughout the sample and must be treated as space-time dependent, $\mathbf{n}(\mathbf{r}, t)$.

In the simplest electro-optic devices a thin layer of liquid crystal is sandwiched between two plates which are each treated in a way which leads to the surface interaction imposing a specified orientation on the liquid crystal. The optical properties of the device can be altered by applying a field whose distorting influence on the liquid crystal opposes that of the surfaces. In all practical cases an electric field is used and it is often found that a critical field exists below which no distortion occurs. The bifurcation defined by this lowest critical field is usually called a Freedericksz transition in the liquid crystal literature. The simplest operating regime for such a device is to switch between two states by the sudden application or removal of an electric field. Hence there are two fundamental questions. First, what is the distortion in each state, and secondly how does the device switch between these?

Determining the behaviour of the director in a liquid crystal device is complicated due to the nature of the material. Liquid crystals are anisotropic and require a large number of material parameters to characterise them. For instance there are at least three coefficients of elasticity, five viscosities and two electric permittivities. In addition there is significant coupling between the material flow and the director distortion, commonly referred to as *back-flow*, particularly during a short transition period.

The static and dynamic behaviour of a simple device is still not fully resolved theoret-

ically even for the well established and simple Twisted Nematic (TN) and SuperTwisted Nematic (STN) devices.

For the static director behaviour the Freedericksz threshold is easy to compute analytically; however, the director structure beyond the threshold is not. At this point it is usual to resort to simulation software [4, 20, 13]. However, analytic solutions would be extremely useful in guiding device development. The bulk behaviour is characterised by the various material constants and practical materials result in a large range of possible values which gives rise to numerous possible different behaviours. As a first step in the systematic investigation of the possible behaviour we consider a case where the elastic constants are nearly equal and where deformations may be modelled in one dimension which means the bifurcation structure is straightforward. More complicated behaviours, involving 'out of plane' distortions [22], crossed electric and magnetic fields [8, 2], etc. remain to be considered in detail.

The dynamics of liquid crystal transitions is also important from a practical point of view as this determines switching times of electro-optic devices. Here the analysis is complicated by the need to account for backflow coupling between the director field and the flow of the liquid. There are many aspects of the dynamics of liquid crystal related to the stable operation of devices, for example bifurcations can be induced by an oscillatory shear [24].

Dynamically, liquid crystal materials can support travelling wave solutions and such solutions are possible in a number of cases as can be seen for example in Lam & Prost [15]. Recently the authors have reported a novel form of travelling wave solution which depends on surface interaction [28]. In addition because of the large number of parameters and spatial variables there are various transient pattern formations possible [14]. Some of these phenomena create areas of analysis that are not primarily motivated by the specific aim of devices improvement but are interesting in their own right.

There are recent devices that utilise more subtle effects in nematic materials, such as the interaction of the nematic with the surface through weak anchoring, but these remain relatively untouched theoretically. There are also new nematic devices which operate in a significantly different manner from the conventional devices. Examples are the use of composites such as Polymer Dispersed Liquid Crystals (PDLC) [5] where small droplets of liquid crystal are held in a solid polymer matrix, and gel systems where a polymer is uniformly dispersed in a much larger fraction of liquid crystal.

In this paper we consider the situation of an initially uniform textured nematic confined between parallel plates and subject to an electric field. The bifurcation structure is easy to understand and we concentrate on obtaining approximate static super-critical solutions using asymptotic techniques. This approach allows approximate descriptions of the static director field to be obtained in a larger variety of situations than previous work. Some extensions to the results are also discussed.

In the next section we describe the continuum theory of nematics and cholesterics. This is followed by a clear statement of the specific problem considered in the rest of the paper. The governing equations are non-dimensionalised and we find that there are three non-dimensional parameters which define the solution. By considering the various physically relevant distinguished limiting cases of these parameters approximate solutions are derived systematically using asymptotic methods. The solutions are presented in both analytic and

numerical form. Hence, we show that methods of modern applied mathematics afford considerable insight into the structure of the solutions of the equations governing liquid crystal device behaviour which have hitherto been regarded as inaccessible to analysis.

2 Continuum theory of nematic liquid crystals

A general account of the theory of liquid crystals can be found in the book by de Gennes & Prost ([6]), and reviews of the continuum theory for nematics and cholesterics in the papers by Ericksen [10] and Leslie [17, 18] and it is inappropriate to give an exhaustive account here. Rather, the aim is to present sufficient theory, amenable to a reader familiar with the continuum theories of Newtonian fluids and linear elastic solids, which will allow for a straightforward physical interpretation.

The main difference between liquid crystal theory and the theory of isotropic liquids arises from the need to include the director field. This results in liquid crystals having a non-symmetric stress tensor and consequently not only the linear momentum equation but also the angular momentum equation is non-trivial. To obtain a mechanical formalism the concept of a couple stress tensor is introduced. This tensor represents torque couplings within the material that are not necessarily produced as the moments of body forces. The equations expressing conservation of momentum and angular momentum can then be written as:

$$\rho \dot{v}_i = F_i + t_{ij,j} + \tilde{t}_{ij,j}, \tag{2.1}$$

$$\sigma \ddot{n}_i = K_i + l_{ij,j} + \varepsilon_{ijk} t_{kj} + \tilde{l}_{ij,k} + \varepsilon_{ijk} \tilde{t}_{kj}. \tag{2.2}$$

Here t_{ij} represents the stress tensor and l_{ij} the couple stress tensor and each has been written as the sum of non-dissipative and dissipative parts with the latter being represented by a superposed tilde, $\tilde{}$. Other terms are: F_i representing a body force; K_i, representing torque acting on the director due to external fields; and v_i the flow velocity. A superposed dot denotes a material time derivative, ρ is the density and σ the director inertia. Subscripted commas denote differentiation with respect to the corresponding spatial variable, ε_{ijk} is the alternating tensor and the summation convention is used.

It is usual, and appropriate, to assume incompressibility and we also note the director n_i is a unit vector. Because of this there are two constraints:

$$v_{i,i} = 0, \qquad n_i n_i = 1, \tag{2.3}$$

which must be satisfied identically. It is also usual to assume that the director inertia is negligible, $\sigma = 0$, and what remains is to exhibit the form of the body couple K_i and the constitutive equations for the stress and couple-stress tensors used in equations (2.1, 2.2).

In the presence of an electric field the couple K_i arises from interaction of the induced dielectric polarisation with the local electric field and has the form

$$K_i = -\varepsilon_{ijk} n_j \frac{\partial W_e}{\partial n_k}, \tag{2.4}$$

where W_e is the electric free energy density given by

$$W_e = -\frac{1}{2}\mathbf{D}\cdot\mathbf{E} = -\frac{1}{2}\varepsilon_0\varepsilon_\perp \mathbf{E}\cdot\mathbf{E} - \frac{1}{2}\varepsilon_0\varepsilon_a(\mathbf{E}\cdot\mathbf{n})^2. \tag{2.5}$$

https://doi.org/10.1017/S0956792501004740 Published online by Cambridge University Press

The electric displacement vector $\mathbf{D}$ is related to the local field $\mathbf{E}$ by $D_i = \varepsilon_{ij}E_j$ and in obtaining (2.5) use has been made of the fact that, for nematics and cholesterics, the permittivity tensor ε_{ij} has only two distinct eigenvalues $\varepsilon_{||}$ and $\varepsilon_{\perp}$ representing the permittivity parallel and perpendicular to the director. The difference of these two, $\varepsilon_a = \varepsilon_{||} - \varepsilon_{\perp}$, is called the electric anisotropy.

The constitutive forms of t_{ij} and l_{ij} are expressed in terms of a distortion free energy density, W_d. The form usually taken for this [11] is

$$W_d = \frac{1}{2}\left(k_1(\nabla\cdot\mathbf{n})^2 + k_2(\tau + \mathbf{n}\cdot(\nabla\times\mathbf{n}))^2 + k_3(\mathbf{n}\times(\nabla\times\mathbf{n}))^2 \right.$$
$$\left. -k_{24}\nabla\cdot\big(\mathbf{n}(\nabla\cdot\mathbf{n}) + \mathbf{n}\times\nabla\times\mathbf{n}\big)\right), \tag{2.6}$$

where the k's are the Frank elastic constants (typically of the order 10^{-12} N). (We follow the notation used by Allender *et al.* [1] for defining the constant k_{24} but note that other authors replace k_{24} by $k_2 + k_{24}$.) The parameter τ is the cholesteric wave number. This expression is the most general scalar function $W_d = W_d(\mathbf{n}, \nabla\mathbf{n})$ which is quadratic in the scalar components of its arguments (essentially an equivalent of Hooke's law), satisfies frame indifference and which is even in the director. (This is required because of the physical equivalence of $\mathbf{n}$ and $-\mathbf{n}$.) For a nematic $\tau = 0$, a reflection of the fact that the pseudo-scalar term must vanish when symmetry is demanded under improper, as well as proper, orthogonal transformations. The four terms in equation (2.6) are each associated with an elementary deformation of the director field and this gives rise to k_1, k_2 and k_3 being known as the splay, twist and bend elastic moduli respectively, while k_{24} is called the saddle-splay modulus (see, for example, Virga [31]).

Whatever constitutive form for W_d is chosen, Ericksen [9] has shown that

$$t_{ij} = -p\delta_{ij} - \frac{\partial W_d}{\partial n_{k,j}}n_{k,i}, \tag{2.7}$$

and

$$l_{ij} = \varepsilon_{ipq}n_p\frac{\partial W_d}{\partial n_{q,j}}. \tag{2.8}$$

The constitutive equations for the dissipative parts of the stress and couple stress tensors $\widetilde{t}_{ij}$ and $\widetilde{l}_{ij}$ were obtained by Leslie [16]. Assuming that they are functions only of n_i, $\dot{n}_i$ and the rate of displacement tensor $v_{i,j}$ and that they satisfy the same invariance conditions as their static counterparts, together with certain linearity assumptions, he concludes that the dissipative couple stress is identically zero: $\widetilde{l}_{ij} \equiv 0$, and that

$$\widetilde{t}_{ij} = +\alpha_1 d_{pq}n_p n_q n_i n_j + \alpha_2 N_i n_j + \alpha_3 N_j n_i + \alpha_4 d_{ij} + \alpha_5 d_{ik}n_k n_j + \alpha_6 d_{jk}n_k n_i. \tag{2.9}$$

In these equations d_{ij} is the symmetric rate of strain tensor and N_i is the covariant director time derivative defined by

$$N_i = \dot{n}_i - \omega_{ij}n_j, \tag{2.10}$$

where $\omega_{ij} = (v_{i,j} - v_{j,i})/2$ is the antisymmetric spin tensor. The α_i are material constants known as Leslie coefficients and have the dimensions of viscosity. Although six in number, only five are independent since a thermodynamic argument by Parodi [23] shows that

$$\alpha_6 - \alpha_5 = \alpha_3 + \alpha_2. \tag{2.11}$$

https://doi.org/10.1017/S0956792501004740 Published online by Cambridge University Press

Defining $W = W_d + W_e$ and

$$g_k = -\gamma_1 N_k - \gamma_2 d_{kp} n_p, \tag{2.12}$$

where

$$\gamma_1 = \alpha_3 - \alpha_2, \qquad \gamma_2 = \alpha_6 - \alpha_5, \tag{2.13}$$

equations (2.1), (2.2) can, after some manipulation, be written as

$$\rho \dot{v}_i = t_{ij,j} + \widetilde{t}_{ij,j}, \tag{2.14}$$

and

$$\left(\frac{\partial W}{\partial n_{i,j}}\right)_{,j} - \frac{\partial W}{\partial n_i} + g_i + \lambda n_i = 0. \tag{2.15}$$

Here λ is an unknown constant (essentially a Lagrange multiplier) arising from the constraint given in the second of equations (2.3). Although it is sometimes helpful to consider the director in terms of its three components $\mathbf{n} = (n_X, n_Y, n_Z)$ for most practical problems it is easier to write it as a function of Euler angles θ^α $(\alpha = 1, 2)$ chosen in such a way that $n_i = n_i(\theta^\alpha)$ satisfies the constraint $n_i n_i = 1$ identically. In this case, the Lagrange multiplier is eliminated and there are only two angular momentum equations.

Having exhibited the dynamic equations in generic form we now consider the boundary equations relevant at solid surfaces and the governing equation for the electric field. The boundary conditions on the velocity will be the usual no-slip conditions. For the director surface conditions are found by equating surface terms arising from divergences in the bulk with variations of a surface energy density, W_s, and of a surface dissipation function, D_s. Making the assumption that neither W_s or D_s depend explicitly spatial derivatives of the director the boundary conditions take the form

$$\frac{\partial W}{\partial \theta_{i,k}} v_k = \frac{\partial W_s}{\partial \theta_i} - \frac{\partial D_s}{\partial \dot{\theta}_i}, \qquad i = 1, 2. \tag{2.16}$$

where v_k is the outward unit normal to the surface and we have written the director in terms of Euler angles. The different forms that can be taken for W_s are discussed in Yokoyama [32] In the literature the limit $W_s \to \infty$ is often taken and this is known as strong anchoring (equivalent to imposing Dirichlet conditions). However, there is increasing interest in weakly anchored systems where finite W_s is assumed. Forms for D_s are considered in Stelzer *et al.* [30] and Sonnet *et al.* [29]. More often than not it is assumed that reorientation at a surface occurs without dissipation, i.e. that D_s is identically zero.

Finally, it is necessary to specify equations determining the electric field. Since we assume no free charge density in the liquid crystal these will be obtained from the Maxwell equations for the electric displacement field

$$\nabla \cdot \mathbf{D} = 0, \tag{2.17}$$

where $\mathbf{D}$ is related to the local field, $\mathbf{E} = -\nabla \Psi$, as discussed above. Boundary conditions are then imposed on the potential Ψ for conducting surfaces and on its normal derivative for insulating surfaces.

https://doi.org/10.1017/S0956792501004740 Published online by Cambridge University Press

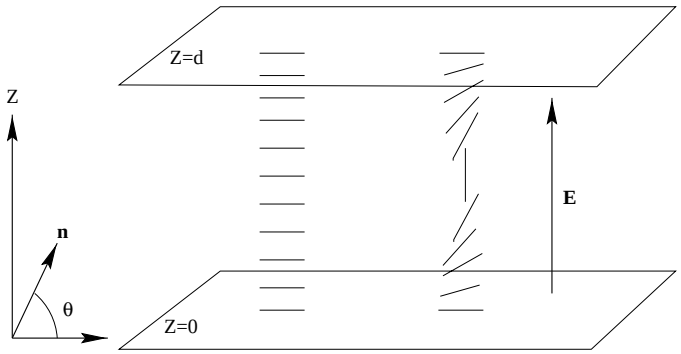

FIGURE 1. Schematic of a simple nematic cell showing the orientation of the director before and after an electric field is applied.

3 A simple nematic cell

We now describe the problem considered in detail in the rest of this paper. We consider a nematic liquid crystal confined between parallel plates at $Z = 0$ and $Z = d$ and subject to strong planar anchoring at these surfaces. An electric potential V_{app} is applied between the plates giving rise to an electric field parallel to the Z-axis, given by an electric potential Ψ. At this point there are several different types of material that could be considered. The most general governing equations of liquid crystal theory are very lengthy and we therefore consider a straightforward case. We will take the liquid crystal as one with positive electric anisotropy, $\varepsilon_a > 0$, so the director tends to align parallel to the local electric field and hence is in competition with the direction of the strong planar anchoring. In addition we will assume the deformation occurs in a plane in which case it is possible to describe the director by one Euler angle alone: $\mathbf{n} = (\cos\theta, 0, \sin\theta)$ where θ is the angle between the director $\mathbf{n}$ and the Z-axis and we assume the distortion depends only on one dimension with $\theta = \theta(Z)$. This situation describes a simple nematic cell, Figure 1. Although this is one of the most straightforward problems which we could have posed it still shows the essentials of more complicated problems and is readily extended to more complicated situations involving weak anchoring, flow coupling, etc. which will be considered elsewhere.

The equations governing the static behaviour of the liquid crystal are obtained from (2.14), (2.15) by suppressing time derivatives. The force equations simply integrate to give an expression for the pressure, while the elastic 'balance of torque' equation is

$$(k_1\cos^2\theta + k_3\sin^2\theta)\frac{d\theta^2}{dZ^2} + (k_3 - k_1)\sin\theta\cos\theta\left(\frac{d\theta}{dZ}\right)^2 + \varepsilon_0\varepsilon_a\cos\theta\sin\theta\left(\frac{d\Psi}{dZ}\right)^2 = 0. \quad (3.1)$$

The Maxwell equation (2.17) written in terms of the electric potential Ψ is

$$\frac{d}{dZ}\left((\varepsilon_\parallel\sin^2\theta + \varepsilon_\perp\cos^2\theta)\frac{d\Psi}{dZ}\right) = 0, \quad (3.2)$$

and the boundary conditions for the problem are

$$\theta(0) = \theta(d) = 0, \qquad \Psi(0) = 0, \quad \Psi(d) = V_{app}. \quad (3.3)$$

https://doi.org/10.1017/S0956792501004740 Published online by Cambridge University Press

The first of these boundary conditions reflects our assumption of strong planar anchoring while the second simply says that the voltage drop across the cell is equal to the applied voltage, V_{app}.

To non-dimensionalise these equations define the scaled variables

$$z = Z/d, \qquad \psi = \Psi/V_{app}, \tag{3.4}$$

so that the problem can be written

$$(1 + \alpha \sin^2\theta)\theta_{zz} + \alpha \sin\theta \cos\theta\, \theta_z^2 + \cos\theta \sin\theta V^2 \psi_z^2 = 0, \tag{3.5}$$

$$\left((1 - \eta \cos^2\theta)\psi_z\right)_z = 0, \tag{3.6}$$

$$\theta(0) = \theta(1) = 0, \qquad \psi(0) = 0, \quad \psi(1) = 1. \tag{3.7}$$

The solution depends upon three non-dimensional parameters defined as

$$\alpha = \frac{k_3}{k_1} - 1, \qquad \eta = 1 - \frac{\varepsilon_\perp}{\varepsilon_\parallel}, \qquad V = \sqrt{\frac{\varepsilon_0 \varepsilon_a}{k_1}}\, V_{app}. \tag{3.8}$$

These are respectively: the non-dimensional elastic anisotropy, the non-dimensional electric anisotropy and the non-dimensional applied voltage.

We shall consider $|\alpha|$ as small. In theory α can take any real value but for many liquid crystals the splay and bend elastic constants have similar values so this assumption is not unreasonable and it is also known that when $|\alpha|$ is large, 'out of plane' distortions can occur. Our assumption of positive anisotropy (which is required to create competition between the applied field and the surface anchoring, restricts η to the range $0 \leqslant \eta < 1$.

The problem always has the trivial solution $\theta = 0$, $\psi = z$ and a simple linear stability analysis shows that this is the only stable solution if $V < V_{crit} = \pi$. Above this critical voltage non-trivial solutions are possible and we must consider non-dimensional voltages in the range $\pi \leqslant V < \infty$. Since we consider α as small there are two parameters that define the various regimes of behaviour and for convenience we take these as $1/V$ and η. If both the non-dimensional parameters are $O(1)$ then we have the full problem and no simplification of the equations can be made and in this case no simple explicit analytic solution exists. However, there are a number of other distinguished limiting cases where approximate analytic solutions can be sought and the six of these that are analysed in this paper are indicated in Figure 2. In Figure 2 the right of the rectangle corresponds to a low applied voltages and will be referred to as the low-field regime. Similarly, the left hand side with $1/V \to 0$ is a high-field regime. As we move up the rectangle from $\eta = 0$ to $\eta = 1$ we move from a low electric anisotropy to a high electric anisotropy regime.

4 Solutions

We consider approximate solutions to the governing equations in the various regimes outlined above. It is worth pointing out that a formal solution by quadrature can always be obtained to the full equations. Such formal solutions (e.g. those by Deuling [7] and Barrat & Fraser [3]) are often used as the starting point for numerical work but do not allow the physical insight which is afforded by an analytic solution. Furthermore, a series solution as an expansion in an appropriate small parameter can more easily be adapted to

https://doi.org/10.1017/S0956792501004740 Published online by Cambridge University Press

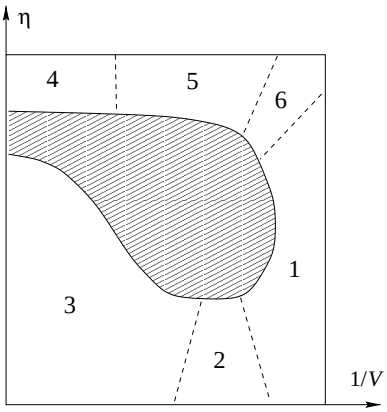

FIGURE 2. Regions of the $(1/V, \eta)$ plane where solutions are sought.

consider the dynamics of the situation. In this paper we obtain such explicit approximate solutions. A fuller account, which also considers some of the possible generalisations, is given in Self [27].

4.1 Low-field regime and small electric anisotropy regime

These cases correspond to Regions 1 and 2 of Figure 2 and we consider them together because their solutions are known elsewhere.

We begin with region 1 where the applied field is low in the sense that $(1/V) \to (1/\pi)^-$ (i.e. just above the Freedericksz transition). Define a small parameter, δ, by writing $(1/V) = (1/\pi) - \delta^2$ and consider $\delta \to 0$. Using standard techniques (e.g. see Logan [21]) the solution can now be found in the form of a regular expansion in δ and we obtain:

$$\theta = \delta \frac{2\sqrt{\pi(1-\eta)}}{\sqrt{1+\alpha(1-\eta)}} \sin \pi z + O(\delta^3), \tag{4.1}$$

$$\psi = z + \delta^2 \frac{\eta}{(1+\alpha(1-\eta))} \sin 2\pi z + O(\delta^4). \tag{4.2}$$

These solutions are illustrated in Figure 3. Notice how the electric field tends to be excluded from the region of maximum distortion. Solutions to the low-field problem have been obtained by Schiller [26].

Region 2 in Figure 2 is characterised by the limit $\eta \to 0$ and is the least amenable limit to analyse. In fact there is no truly simplifying approximate solution and a result is obtained in the form of elliptic integrals, i.e. a formal solution by quadrature. In practical terms more progress is made by breaking this region into two – a region $1/V \to 1/\pi$ which is covered by the low field regime presented in the last section, and a region $1/V \to 0$ (corresponding to a high applied field) discussed in the next section below. However, the regime considered here is required for completeness since it is the distinguished limit and hence matches the other two. We therefore present the formal solution to leading order.

From the second equation of (3.8) it is evident that the limit $\eta \to 0$ is equivalent to $\varepsilon_a \to 0$ and this implies that the internal electric field is very nearly equal to the applied field. Such a characteristic is more common in the physical properties associated with

https://doi.org/10.1017/S0956792501004740 Published online by Cambridge University Press

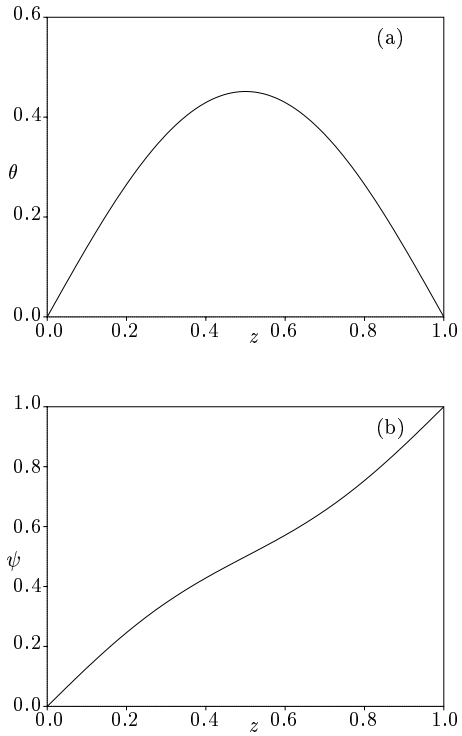

FIGURE 3. Solutions in the low field regime. (a) the distortion angle θ, (b) the electric potential ψ. Parameter values used are: $V = 1.2\pi$, $\eta = 0.75$, $\alpha = 0$.

liquid crystal's response to a magnetic field and we therefore refer to this limit as the *magnetic approximation*. Putting $\eta = 0$ in the Maxwell equation (3.6) we obtain the leading order potential $\psi_0 = z$. Substituting into equation (3.5) and assuming a symmetric solution we formally integrate to obtain θ implicitly from:

$$z = \frac{1}{V}\int_0^{\theta} (1 + \alpha \sin^2 w \sin^2 \theta_m)^{\frac{1}{2}}(1 - \sin^2 \theta_m \sin^2 w)^{-\frac{1}{2}} \sin\theta_m \, dw, \tag{4.3}$$

with the maximum distortion angle, θ_m, being given by the elliptic integral:

$$V = \int_0^{\frac{\pi}{2}} (1 + \alpha \sin^2 w \sin^2 \theta_m)^{\frac{1}{2}}(1 - \sin^2 \theta_m \sin^2 w)^{-\frac{1}{2}} \sin\theta_m \, dw. \tag{4.4}$$

This solution has been given by Deuling [7].

4.2 High-field low electric anisotropy regime

In this and the next section, we consider cases where a high field is applied. This is a common situation encountered in practice since high fields are employed to decrease switching times. In this section we consider a parameter range corresponding to region 3 of Figure 2, that is, a high field applied to a liquid crystal with a small electric anisotropy.

https://doi.org/10.1017/S0956792501004740 Published online by Cambridge University Press

The new solution given in this section is in the form of a matched asymptotic expansion and we demonstrate its robustness when parameter values are changed. From the point of view of applicability this is the most important result of the paper.

Because the applied field is high we introduce a parameter ϵ defined by

$$\epsilon = 1/V \tag{4.5}$$

and consider the limit $\epsilon \to 0$. Region 3 is also characterised by small η and we also assume α is small. The distinguished limit in this case corresponds to the scalings

$$\eta = \epsilon\overline{\eta}\,,\ \alpha = \epsilon\overline{\alpha}, \tag{4.6}$$

where $\overline{\eta}$ and $\overline{\alpha}$ are both $O(1)$. The governing equations (3.5) and (3.6) are now

$$\epsilon^2\left(\epsilon\overline{\alpha}\sin^2\theta + 1\right)\theta_{zz} + \epsilon^3\overline{\alpha}\sin\theta\cos\theta\,\theta_z^2 + \sin\theta\cos\theta\,\psi_z^2 = 0, \tag{4.7}$$

$$\left((1 - \epsilon\overline{\eta}\cos^2\theta)\psi_z\right)_z = 0, \tag{4.8}$$

with the boundary conditions (3.7). This is a singular limit of the problem and we expect an *outer solution* in most of the interior together with thin *inner solutions* being boundary layers adjacent to the confining surfaces. We obtain these in the series form and are also able to obtain an overall composite solution.

4.2.1 *Outer problem*

In the outer region with $z = O(1)$ we expand

$$\theta = \theta_0 + \epsilon\theta_1 + \epsilon^2\theta_2 + \ldots \qquad \psi = \psi_0 + \epsilon\psi_1 + \epsilon^2\psi_2 + \ldots. \tag{4.9}$$

Substituting these expansions into (4.7) and (4.8) we find that any integer multiple of $\pi/2$ satisfies the outer problem. We take the physically relevant outer solution:

$$\theta_0 = \pi/2\,, \qquad \theta_n = 0 \qquad n \geqslant 1, \tag{4.10}$$

and

$$\psi_0 = C_0 z + B_0, \quad \psi_1 = C_1 z + B_1, \quad \psi_2 = \ldots \quad \text{etc.} \tag{4.11}$$

The constants C_n, B_n will be determined by matching the inner and outer solutions.

4.2.2 *Inner problems*

It is apparent that the outer solution for θ cannot satisfy the boundary conditions $\theta(0) = \theta(1) = 0$ and we therefore expect boundary layers close to $z = 0$ and $z = 1$. In these regions, θ changes rapidly and we seek a new balance in equation (4.7) by re-scaling z. To make the second derivative term $O(1)$ the correct re-scalings to use are $z = \epsilon\overline{z}$ for the left region and $z = 1 - \epsilon\overline{z}$ for the right region. In each case, $\overline{z} = O(1)$. The governing equations become

$$\epsilon^2(\epsilon\overline{\alpha}\sin^2\overline{\theta} + 1)\overline{\theta}_{\overline{z}\overline{z}} + \epsilon^3\overline{\alpha}\sin\overline{\theta}\cos\overline{\theta}\,\overline{\theta}_{\overline{z}}^2 + \sin\overline{\theta}\cos\overline{\theta}\,\overline{\psi}_{\overline{z}}^2 = 0, \tag{4.12}$$

$$\left(1 - \epsilon\overline{\eta}\cos^2\overline{\theta})\overline{\psi}_{\overline{z}}\right)_{\overline{z}} = 0. \tag{4.13}$$

https://doi.org/10.1017/S0956792501004740 Published online by Cambridge University Press

Overbars on θ and ψ denote that they are functions of the inner variable $\bar{z}$. We expand as before and substitute into (4.12) and (4.13). Working to $O(\epsilon^2)$ the equations for $\overline{\psi}$ in the left inner region are:

$$\overline{\psi}_{0\bar{z}} = \overline{C}_0, \tag{4.14}$$

$$\overline{\psi}_{1\bar{z}} = \overline{C}_1, \tag{4.15}$$

$$\overline{\psi}_{2\bar{z}} = \overline{C}_2 + \overline{\eta}\,\overline{C}_1 \cos^2\overline{\theta}_0; \tag{4.16}$$

while for $\overline{\theta}$ we have at $O(1)$ and at $O(\epsilon)$:

$$\overline{\theta}_{0\bar{z}\bar{z}} + \overline{C}_1^2\,\cos\overline{\theta}_0 \sin\overline{\theta}_0 = 0, \tag{4.17}$$

$$\overline{\theta}_{1\bar{z}\bar{z}} + \overline{C}_1^2 \cos 2\overline{\theta}_0\,\overline{\theta}_1 = 2\overline{\eta}\cos^2\overline{\theta}_0\,\overline{\theta}_{0\bar{z}\bar{z}} - 2\overline{C}_1\overline{C}_2\cos\overline{\theta}_0\sin\overline{\theta}_0 - \overline{\alpha}(\sin^2\overline{\theta}_0\,\overline{\theta}_{0\bar{z}\bar{z}} + \sin\overline{\theta}_0\cos\overline{\theta}_0\,\overline{\theta}_{0\bar{z}}^2). \tag{4.18}$$

Equations (4.14) and (4.15) together with the appropriate boundary conditions give

$$\overline{\psi}_0 = 0, \qquad \text{and} \qquad \overline{\psi}_1 = \overline{C}_1\bar{z}. \tag{4.19}$$

The leading order equation (4.17) clearly integrates once and by demanding that the derivative $\overline{\theta}_{\bar{z}}$ match with that of the outer solution, so $\bar{z} \to \infty$ implies $\overline{\theta}_0 \to \pi/2$, $\overline{\theta}_{0\bar{z}} \to 0^+$, we conclude the integration constant is zero. A further integration gives the solution for $\overline{\theta}$ satisfying the boundary condition $\overline{\theta}(0) = 0$ as

$$\overline{\theta}_0 = 2\tan^{-1}(e^{\overline{C}_1\bar{z}}) - \frac{\pi}{2}. \tag{4.20}$$

Next, the second order equation, (4.16), together with the boundary condition $\overline{\psi}_2(0) = 0$ gives

$$\overline{\psi}_2 = +\overline{C}_2\bar{z} + \overline{\eta}\tanh(\overline{C}_1\bar{z}). \tag{4.21}$$

Collecting together the above results we have expressions for the electric potential ψ in the left inner region to $O(\epsilon^2)$. This solution must smoothly match with the outer solution (4.11). We use Van Dyke's matching rule, as quoted in standard texts on asymptotics (e.g. Hinch [12]) to determine the constants involved and find:

$$\overline{\psi}^l = \quad \epsilon\bar{z} + \epsilon^2\overline{\eta}\tanh\bar{z} + O(\epsilon^3), \tag{4.22}$$

$$\psi^o = \quad z - \epsilon^2\overline{\eta}(2z-1) + O(\epsilon^3), \tag{4.23}$$

$$\overline{\psi}^r = 1 - \epsilon\bar{z} - \epsilon^2\overline{\eta}\tanh\bar{z}) + O(\epsilon^3). \tag{4.24}$$

Finally, we are now able to solve for the director field in the inner region at $O(\epsilon)$ by integrating equation (4.18). We obtain

$$\overline{\theta}_1 = \frac{1}{2}\overline{\alpha}\,(\tanh\bar{z} - \bar{z})\,\mathrm{sech}\bar{z} + \frac{1}{2}\overline{\eta}\ \tanh\bar{z}\,\mathrm{sech}\bar{z}. \tag{4.25}$$

It is straightforward to find analogous solutions for θ in the right inner region since the solution is symmetric in z. To complete the solution we obtain composite expansions for θ and ψ using the standard procedure (again, see Hinch [12]), and obtain

$$\psi^c = z + \epsilon^2\overline{\eta}\tanh\frac{z}{\epsilon} - \epsilon^2\overline{\eta}\tanh\frac{1-z}{\epsilon} - \epsilon^2(2z-1)\overline{\eta} + O(\epsilon^3), \tag{4.26}$$

https://doi.org/10.1017/S0956792501004740 Published online by Cambridge University Press

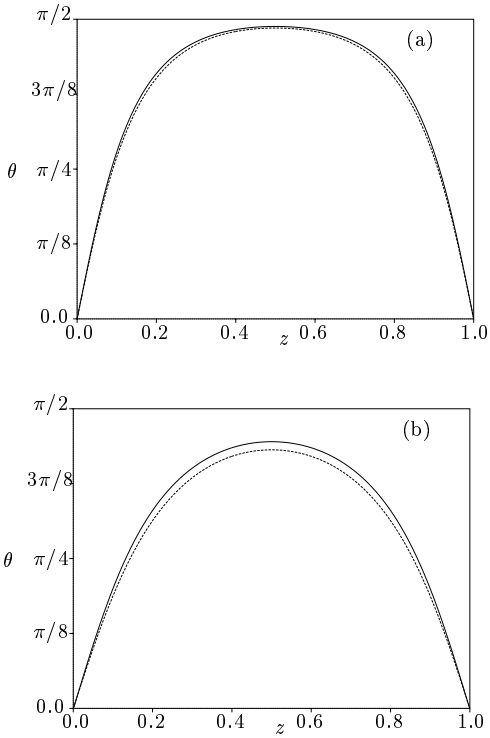

FIGURE 4. Composite solutions for the distortion angle θ, in the high-field low-anisotropy regime. Parameter values used are: $\alpha = 0.1$, $\eta = 0.2$, and in (a) $V = 3\pi$, while in (b) $V = 2\pi$. Solid curves are the analytic expressions and dashed curves are the numerical solutions.

$$\begin{aligned}\theta^c \sim\ & 2\tan^{-1}(e^{z/\epsilon}) + 2\tan^{-1}(e^{(1-z)/\epsilon}) - 3\pi/2 \\ & + \frac{1}{2}\epsilon\bar{\alpha}\left(\tanh\frac{z}{\epsilon} - \frac{z}{\epsilon}\right)\operatorname{sech}\frac{z}{\epsilon} + \frac{1}{2}\epsilon\bar{\eta}\tanh\frac{z}{\epsilon}\operatorname{sech}\frac{z}{\epsilon} \\ & + \frac{1}{2}\epsilon\bar{\alpha}\left(\tanh\frac{1-z}{\epsilon} - \frac{1-z}{\epsilon}\right)\operatorname{sech}\frac{1-z}{\epsilon} + \frac{1}{2}\epsilon\bar{\eta}\tanh\frac{1-z}{\epsilon}\operatorname{sech}\frac{1-z}{\epsilon}. \quad (4.27)\end{aligned}$$

In Figures 4 and 5 these analytic expressions are compared with the numerical solutions of equations (4.7) and (4.8) for various values of the parameters. In Figure 4 the composite distortion is shown at two and three times the critical voltage. The potential is not shown since, under these conditions, the composite analytic solution is almost indistinguishable from the numerical solution. The robustness of the approximate analytic solutions in this limit can be seen in Figure 5 where the applied voltage is only three times the critical voltage and the parameters used are those of liquid crystal E7 (see, for example, Preist *et al.* [25]). In this case both the electric and elastic anisotropies are high ($\eta = 0.73$ and $\alpha = 0.62$), but despite this there is still good agreement between the analytic and numerical solutions.

https://doi.org/10.1017/S0956792501004740 Published online by Cambridge University Press

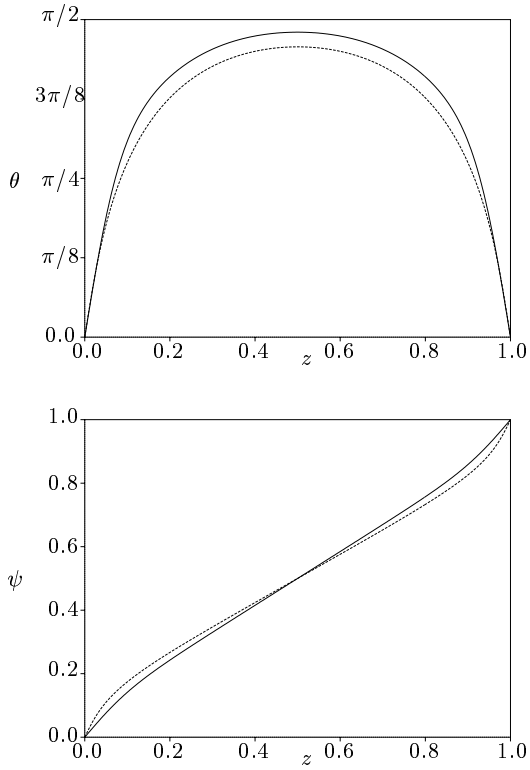

FIGURE 5. Composite solutions for the distortion angle θ, and electric potential ψ, in the high-field low-anisotropy regime. Parameter values used are: $\alpha = 0.62$, $\eta = 0.73$, $V = 3\pi$. Solid curves are the analytic expressions and dashed curves are the numerical solutions.

4.2.3 *Discussion*

Having considered the case of high-field and low electric anisotropy the natural situation to consider next is that of larger anisotropy, that is moving up in Figure 2 from the bottom left corner. As the magnitude of the anisotropy increases the solution retains the same boundary layer structure as above. However, when $\eta = O(1)$ the full problem arises in the boundary layer and we do not present any results for this case. In Figure 2 we have left this region shaded to indicate the lack of a simplifying solution and we have also indicated that the results of region 3 appear to give very reasonable predictions for a significant range of η. As η is further increased a new balance in the equations occurs allowing progress to be made analytically and this is discussed in the next section.

4.3 High-field, large electric anisotropy regime

In this and the next two subsections we consider cases where the electric anisotropy is large and the applied field is taken as being respectively, high, intermediate, and low. These correspond to regions 4, 5 and 6 in Figure 2. In each case we present the solution to leading order and we find that, for the case where α is small, this parameter does not appear in the solution to lowest order. Consequently, α is not included in the following

https://doi.org/10.1017/S0956792501004740 Published online by Cambridge University Press

analysis. The high anisotropy of the electric permittivity implies we are assuming that $\eta \sim 1$ so define

$$\gamma = 1 - \eta = \frac{\varepsilon_\perp}{\varepsilon_{||}} \tag{4.28}$$

and consider the limit $\gamma \to 0$.

We begin in this section with the high-field regime of Region 4 in figure 2 and we again define a small parameter ϵ as the reciprocal applied voltage (4.5). In terms of ϵ and γ and with $\alpha = 0$ equations (3.5) and (3.6) become

$$\epsilon^2 \theta_{zz} + \frac{C^2 \sin\theta \cos\theta}{\left(\sin^2\theta + \gamma\cos^2\theta\right)^2} = 0, \qquad \psi_z = \frac{C}{\sin^2\theta + \gamma\cos^2\theta}. \tag{4.29}$$

We have integrated the Maxwell equation once so C is a constant and the boundary conditions are again given by (3.7). We wish to solve in the limit $\epsilon \to 0$. The distinguished limit we are considering is defined by the relative order of magnitude of γ compared to ϵ. This appears naturally during the analysis and is discussed below. To solve this problem to arbitrary order we would expand C in powers of ϵ but to the order we will solve here we need only consider the leading term. For a physically sensible analysis, we must take this as being non-zero and we therefore assume $C = O(1)$.

4.3.1 *Outer problem*

The leading order outer problem clearly has solutions

$$\theta = \frac{\pi}{2}, \qquad \text{and} \qquad \psi = Cz + B. \tag{4.30}$$

4.3.2 *Inner problems*

As before define the inner regions by rescaling $z = \epsilon\bar{z}$ and $z = 1 - \epsilon\bar{z}$ in the left and right boundary layers respectively. In this case, it is convenient to rescale the potential in the inner regions by defining

$$\psi^l = \epsilon\overline{\psi}^l, \qquad \psi^r = 1 - \epsilon\overline{\psi}^r. \tag{4.31}$$

and this gives the inner equations

$$\overline{\theta}_{\bar{z}\bar{z}} = -\frac{C^2 \sin\overline{\theta}\cos\overline{\theta}}{\left(\sin^2\overline{\theta} + \gamma\cos^2\overline{\theta}\right)^2}, \qquad \overline{\psi}_{\bar{z}} = \frac{C}{\sin^2\overline{\theta} + \gamma\cos^2\overline{\theta}}, \tag{4.32}$$

where the superscripts l and r have been dropped because the equations are identical in the two inner regions. Putting $\gamma = 0$ in the first of (4.32) gives the leading order solution

$$\overline{\theta} = \cos^{-1}\left(be^{-C\bar{z}}\right). \tag{4.33}$$

Clearly, this matches correctly with the outer solution, and the boundary condition $\overline{\theta}(0) = 0$ appears to imply that $b = 1$. However, note that from (4.33) $\overline{\theta}_{\bar{z}} \to \infty$ as $\bar{z} \to 0$. Thus the problem is again singular and an inner-inner region exists. When discussing this new region below it will be shown that $b = 1$ is in fact correct. Anticipating this we

https://doi.org/10.1017/S0956792501004740 Published online by Cambridge University Press

therefore take $b = 1$ in equation (4.33) and obtain the leading order solution for $\overline{\psi}$ as

$$\overline{\psi} = \frac{1}{2}\log(e^{2C\overline{z}} - 1) + E. \tag{4.34}$$

4.3.3 *Inner-inner problems*

There is a need to find a new balance as $\overline{z} \to 0$ in order to avoid an infinite derivative. In the denominators of equations (4.32) we have $\gamma \cos^2\overline{\theta} \sim \sin^2\overline{\theta}$ when $\overline{\theta} = O(\sqrt{\gamma})$. To find where this occurs expand (4.33) for small $\overline{\theta}$, $\overline{z}$:

$$1 - \frac{\overline{\theta}^2}{2} \sim b - bC\overline{z}. \tag{4.35}$$

To balance at $O(1)$ we must clearly put $b = 1$ as anticipated above. Balancing at first order in small quantities it is seen that $\overline{\theta} = O(\sqrt{\gamma})$ when $\overline{z} = O\left(\gamma/2C\right)$. Thus the appropriate scalings to use in the inner-inner regions (denoted by a circumflex) are

$$\overline{z} = \frac{\gamma}{2C}\widehat{z} \qquad \text{and} \qquad \overline{\theta} = \sqrt{\gamma}\widehat{\theta}. \tag{4.36}$$

In terms of these variables the leading order inner-inner equations are

$$\widehat{\theta}_{\widehat{z}\widehat{z}} = \frac{-\widehat{\theta}}{4\left(1 + \widehat{\theta}^2\right)^2} \qquad \text{and} \qquad \widehat{\psi}_{\widehat{z}} = \frac{1}{2\left(1 + \widehat{\theta}^2\right)}. \tag{4.37}$$

The first of these can be integrated once and smooth matching of the derivative θ_z as we move from inner-inner to inner regions determines the integration constant. Integrating again and applying the boundary conditions $\widehat{\theta}(0) = 0$ gives

$$\widehat{z} = \widehat{\theta}\sqrt{\widehat{\theta}^2 + 1} + \sinh^{-1}\widehat{\theta}. \tag{4.38}$$

It will be useful to introduce some notation for this implicit function and hence we call the left side of (4.38) $\mathscr{P}^{-1}\left(\widehat{\theta}\right)$ and we then have the formal solution

$$\widehat{\theta} = \mathscr{P}(\widehat{z}). \tag{4.39}$$

To determine the potential, $\widehat{\psi}$, to leading order we note that

$$\widehat{\psi}_{\widehat{z}} = \frac{\partial\widehat{\psi}}{\partial\widehat{\theta}}\frac{d\widehat{\theta}}{d\widehat{z}}, \tag{4.40}$$

and hence obtain the solution in each inner boundary layer as

$$\widehat{\psi} = \sinh^{-1}\widehat{\theta}. \tag{4.41}$$

4.3.4 *Matching the solutions*

The scalings used and the solutions found above are summarized in Table 1. The constants in these solutions are found by matching ψ using the asymptotic behaviour in the appropriate limits for the various regions. We obtain:

$$B \sim \epsilon\log 2 - \tfrac{1}{2}\epsilon\log\gamma, \tag{4.42}$$

https://doi.org/10.1017/S0956792501004740 Published online by Cambridge University Press

Table 1. *Summary of scalings and solutions in the different regions*

Left inner-inner	Left inner	Outer	Right inner	Right inner-inner
$\overline{z} = \frac{\gamma}{2C}\widehat{z}$	$z = \epsilon\overline{z}$	z	$z = 1 - \epsilon\overline{z}$	$\overline{z} = \frac{\gamma}{2C}\widehat{z}$
$\overline{\theta} = \sqrt{\gamma}\widehat{\theta}$	$\overline{\theta} = \theta$	θ	$\overline{\theta} = \theta$	$\overline{\theta} = \sqrt{\gamma}\widehat{\theta}$
$\widehat{\psi} = \overline{\psi}$	$\psi = \epsilon\overline{\psi}$	ψ	$\psi = 1 - \epsilon\overline{\psi}$	$\widehat{\psi} = \overline{\psi}$
$\widehat{\theta} \sim \mathscr{P}(\widehat{z})$	$\overline{\theta} \sim \cos^{-1}(e^{-C\overline{z}})$	$\theta \sim \frac{\pi}{2}$	$\overline{\theta} \sim \cos^{-1}(e^{-C\overline{z}})$	$\widehat{\theta} \sim \mathscr{P}(\widehat{z})$
$\widehat{\psi} \sim \sinh^{-1}\widehat{\theta}$		$\psi \sim Cz + B$		$\widehat{\psi} \sim \sinh^{-1}\widehat{\theta}$
	$\overline{\psi} \sim \frac{1}{2}\log(e^{2C\overline{z}} - 1) + E$		$\overline{\psi} \sim \frac{1}{2}\log(e^{2C\overline{z}} - 1) + F$	

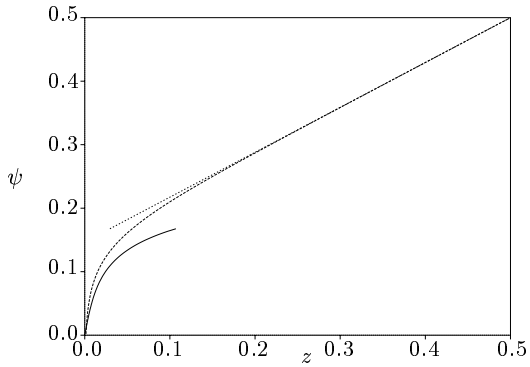

FIGURE 6. The potential, ψ, in the high-field large-anisotropy regime showing outer, inner and inner-inner solutions. Parameter values used are: $\alpha = 0.0$, $\gamma = 0.1$, $V = 4\pi$.

$$C \sim 1 - 2\epsilon + \epsilon\log\gamma, \tag{4.43}$$

$$E \sim \log 2 - \tfrac{1}{2}\log\gamma, \tag{4.44}$$

$$F \sim \log 2 - \tfrac{1}{2}\log\gamma. \tag{4.45}$$

The constants as written here are in fact expanded in terms of the parameters ϵ and γ. This has arisen because of the need to rescale the dependent, as well as independent, variables in the various regions. We also note that E and F occur in the expressions for $\overline{\psi}$ which, in each case, is scaled with ϵ. Thus the parameter γ appears in the *unscaled* variables only in the combination $\epsilon\log\gamma$. Recalling that $C = O(1)$ we see that the distinguished limit is defined by

$$\epsilon|\log\gamma| \ll 1, \tag{4.46}$$

and this defines what is meant by a *high-field* in the high-anisotropy regime. As $\gamma \to 0$ an increasingly high (non-dimensional) field is required to cause saturation. This is discussed further in the following section.

Because of the implicit nature of the inner-inner solutions, it is not possible to write down the composite solution explicitly. An illustration of the boundary layer structure for the potential in this regime is shown in Figure 6.

https://doi.org/10.1017/S0956792501004740 Published online by Cambridge University Press

4.4 Intermediate-field large electric anisotropy regime

This regime corresponds to region 5 of Figure 2 and, as in the previous section, we consider the limit $\gamma \to 0$. We do not, however, take the applied voltage as being *high*. We shall find that the structure of the solution requires boundary layers but that, in addition, the solution in each layer interacts with the solutions in all other regions indicating a delicate balance between the various physical processes in the problem. We view this regime as the most mathematically interesting of all those considered in this paper.

The previous section describes a limiting case of the present regime where the applied field is sufficiently high to cause saturation of the director field, i.e. an outer solution $\theta = \pi/2$ exists. In the present case, V is not sufficiently large and the outer solution attains a maximum distortion $\theta_m < \pi/2$. The structure of the outer solution is similar to that of the inner regions of the previous section and, similarly, the boundary layers here have a structure similar to the inner-inner solutions. In the last section, it was shown that for saturation to occur the applied voltage must satisfy $V \gg |\log\gamma|$. We may, therefore, naively suppose that the present regime corresponds to $V = O(|\log\gamma|)$ and this is indeed the case as will be shown below. As before when α is small it does not affect the lowest order solution so again we will not consider it in the analysis. The governing equations can then be written as

$$\theta_{zz} + \frac{C^2V^2\sin\theta\cos\theta}{\left(\sin^2\theta + \gamma\cos^2\theta\right)^2} = 0, \qquad \psi_z = \frac{C}{\sin^2\theta + \gamma\cos^2\theta}. \tag{4.47}$$

By putting $\gamma = 0$ and assuming symmetric solutions with $\theta = \theta_m$ and $\psi = 1/2$ at $z = 1/2$, (where θ_m is unknown), gives the leading order outer solutions

$$\cos\theta = \cos\theta_m \cosh\left\{(z - \frac{1}{2})\frac{CV}{\sin\theta_m}\right\}, \tag{4.48}$$

$$\psi = \frac{1}{2V}\log\left(\sin\theta_m + \tanh\left\{(z-\frac{1}{2})\frac{CV}{\sin\theta_m}\right\}\right) + \frac{1}{2} - \frac{1}{2V}\log\left(\sin\theta_m - \tanh\left\{(z-\frac{1}{2})\frac{CV}{\sin\theta_m}\right\}\right). \tag{4.49}$$

4.4.1 *Inner problems*

Examining equations (4.47) the outer region approximation breaks down when $\theta \sim \sqrt{\gamma}$. Thus we scale $\theta = \sqrt{\gamma}\bar{\theta}$ and determine the value of z where this first occurs by expanding equation (4.48) for small $\theta = \sqrt{\gamma}\bar{\theta}$ and z. Demanding the resulting expansions balance at each order requires:

$$1 = \cos\theta_m \cosh\left\{\frac{CV}{2\sin\theta_m}\right\}, \tag{4.50}$$

and

$$\frac{\gamma\bar{\theta}^2}{2} \sim z\frac{CV\cos\theta_m}{\sin\theta_m}\sinh\left\{\frac{CV}{2\sin\theta_m}\right\}. \tag{4.51}$$

The first of these gives an expression for C in terms of the applied voltage V and the maximum distortion θ_m. (Strictly, equality only holds in the limit $\gamma \to 0$.) On substituting

https://doi.org/10.1017/S0956792501004740 Published online by Cambridge University Press

(4.50) and manipulating (4.51) the correct scaling to use for the inner variable is

$$z = \frac{\gamma}{2CV}\bar{z}, \tag{4.52}$$

and the inner equations can be written to leading order as

$$\bar{\theta}_{\bar{z}\bar{z}} = \frac{-\bar{\theta}}{4(1+\bar{\theta}^2)^2}, \qquad \bar{\psi}_{\bar{z}} = \frac{1}{2V(1+\bar{\theta}^2)}. \tag{4.53}$$

Analogously to the the previous section we find

$$\bar{\theta} = \mathscr{P}(\bar{z}), \qquad \bar{\psi} = \frac{1}{V}\sinh^{-1}\bar{\theta}, \tag{4.54}$$

where the function $\mathscr{P}$ is again defined by (4.38) and (4.39). An analogous argument for the limit $z \to 1$ shows that in the right boundary layer we must rescale $z = 1 - \frac{\gamma}{2CV}\bar{z}$. We then obtain the first of (4.54) as the solution for $\bar{\theta}$ and for the potential we obtain $\bar{\psi} = 1 - (1/V)\sinh^{-1}\bar{\theta}$.

4.4.2 *Matching the solutions*

We note θ is already matched by the relationship (4.50). To match the potential begin by rearranging (4.50) as:

$$\tanh\frac{CV}{2\sin\theta_m} = \sin\theta_m. \tag{4.55}$$

(Given this result it is easier to see the singular character of the outer solution for ψ given by equation (4.49) at the two end points $z = 0$ and $z = 1$.) Substituting (4.55) in (4.49) for ψ we obtain the expansion of the outer solution as $z \to 0$:

$$\psi \sim \frac{1}{2V}\log\left(\frac{CV}{2}\cot^2\theta_m\right) + \frac{1}{2} + \frac{1}{2V}\log z. \tag{4.56}$$

We must also determine the behaviour of the inner solution for the potential (4.54) as $\bar{z} \to \infty$. This solution is of the form $\bar{\psi} = \bar{\psi}(\bar{\theta})$ and from (4.54) and the definition of $\mathscr{P}$ we obtain

$$\bar{\theta} \sim \sqrt{\bar{z}} - \frac{\log\bar{z}}{2\sqrt{\bar{z}}} - \frac{1}{4\sqrt{\bar{z}}}(1 + 2\log 2) + \ldots \qquad \text{as} \qquad \bar{z} \to \infty. \tag{4.57}$$

Substituting this into (4.54) for $\bar{\psi}$ we obtain:

$$\bar{\psi} \sim \frac{1}{V}\log 2\sqrt{\bar{z}} \qquad \text{as} \qquad \bar{z} \to \infty. \tag{4.58}$$

Comparing this with (4.56) and using (4.50) we obtain

$$\tan\theta_m = \frac{\sqrt{\gamma}}{4}e^{V/2}, \tag{4.59}$$

and this constitutes the final matching condition. The inner and outer solutions are compared with the numerical solutions in Figure 7.

As in the last subsection it is not possible to obtain an analytic expression for the composite solution although this is easy to obtain numerically (Figure 8).

https://doi.org/10.1017/S0956792501004740 Published online by Cambridge University Press

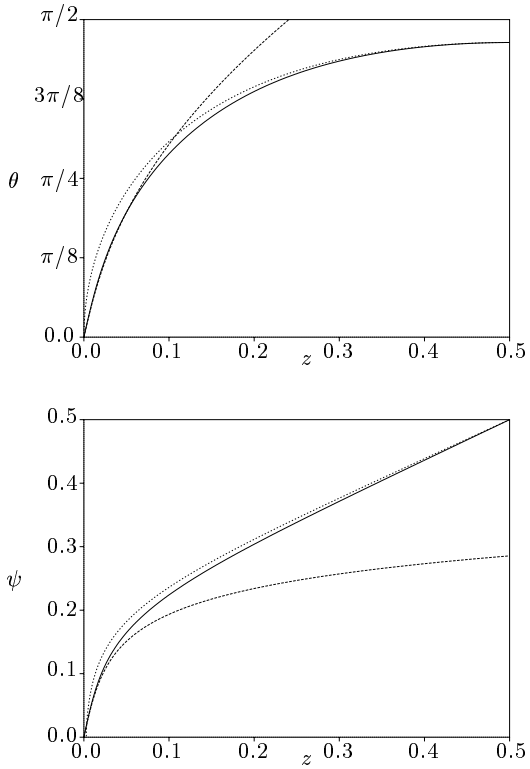

FIGURE 7. Solutions for the distortion angle θ, and electric potential ψ, in the intermediate-field high-anisotropy regime. Parameter values used are: $\gamma = 0.1$, $V = 2\pi$. Dashed curves are the inner and outer analytic expressions and solid curves are the numerical solutions.

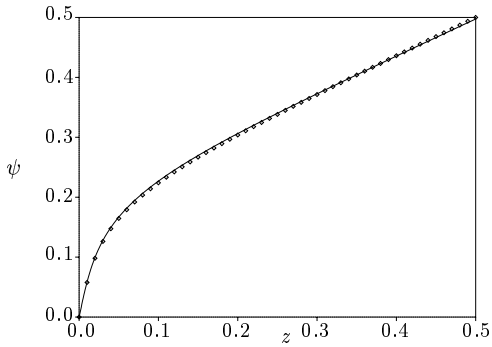

FIGURE 8. Solutions for the electric potential ψ, in the intermediate-field high-anisotropy regime. Parameter values used are: $\gamma = 0.1$, $V = 2\pi$. The solid curve is the composite solution and symbols are the numerical solution.

https://doi.org/10.1017/S0956792501004740 Published online by Cambridge University Press

4.4.3 *Discussion*

The constants θ_m and C which appear in the inner and outer solutions which were obtained from the matching conditions determine not just the limiting behaviour in the overlap region but also the overall shape of the solutions. It is evident from (4.59) that for significant distortion to occur, i.e. $\theta_m = O(1)$, the applied voltage must satisfy

$$V = O(1) - \log\gamma. \tag{4.60}$$

This is consistent with the analysis of the previous section where it was shown that, for saturation to occur, the voltage must be so high that $V \gg -\log\gamma$. We also note that, as $\gamma \to 0$, even $O(1)$ voltages can be considered small. However, equation (4.59) predicts a finite distortion for $V \to 0$ which is indicative of asymptotic breakdown. Thus for 'low' voltages we must seek a new balance in the equations.

4.5 Low-field, large electric anisotropy regime

The final large electric anisotropy regime is region 6 of Figure 2 and lies between the intermediate-field regime of the last subsection and and the low-field limit considered in § 5.1. There is little of practical interest in the solution presented other than it allows proper matching of these two other solutions. It is characterised by $\gamma \to 0$ and $V \to \pi$. The governing equations are identical to those used in the previous section, (4.47), but a different solution is obtained since we scale the equations at the outset. It was shown above that relatively high fields are required to obtain an appreciable distortion because the limit $\gamma \to 0$ defines a regime where large polarisation changes can be induced by even a relatively small distortion of the director field. Consequently, for relatively low fields any distortion of the director must be assumed small. The correct distinguished limit is therefore obtained by rescaling

$$\theta = \sqrt{\gamma}\overline{\theta}, \quad \text{and} \quad C = \gamma\overline{C}, \tag{4.61}$$

and this gives the following equations to leading order:

$$\overline{\theta}_{zz} + \overline{C}^2 V^2 \frac{\overline{\theta}}{(1+\overline{\theta}^2)^2} = 0, \qquad \psi_z = \frac{\overline{C}}{1+\overline{\theta}^2}. \tag{4.62}$$

Assuming a symmetric solution these are integrable in terms of elliptic functions:

$$\frac{1}{V\overline{C}}(1+\overline{\theta}_m^2)\left\{\mathrm{E}(\tfrac{\pi}{2},k) - \mathrm{E}(\phi,k)\right\} = \begin{cases} z, & z < 1/2; \\ 1-z, & z \geqslant 1/2, \end{cases} \tag{4.63}$$

$$\psi = \begin{cases} \frac{1}{V}\left(\mathrm{F}(\frac{\pi}{2},k) - \mathrm{F}(\phi,k)\right), & z < 1/2 \\ 1 - \frac{1}{V}\left(\mathrm{F}(\frac{\pi}{2},k) - \mathrm{F}(\phi,k)\right). & z \geqslant 1/2 \end{cases} \tag{4.64}$$

In these equations $\mathrm{F}(\phi,k)$ and $\mathrm{E}(\phi,k)$ are elliptic integrals of the first and second kind respectively and

$$k^2 = \frac{\overline{\theta}_m^2}{1+\overline{\theta}_m^2}, \qquad \phi = \cos^{-1}\left(\frac{\overline{\theta}}{\overline{\theta}_m}\right) \qquad \text{and} \qquad \frac{1}{V\overline{C}}(1+\overline{\theta}_m^2)\mathrm{E}(\tfrac{\pi}{2},k) = \tfrac{1}{2}. \tag{4.65}$$

https://doi.org/10.1017/S0956792501004740 Published online by Cambridge University Press

The constants in the problem are determined by exploiting the symmetry of the solution. Substituting $z = 1/2, \overline{\theta} = \overline{\theta}_m$ and $\psi = 1/2$ into (4.64) we obtain the algebraic equation:

$$\frac{V}{2} = \mathrm{F}(\tfrac{\pi}{2}, k) = \mathrm{K}(k), \tag{4.66}$$

where $\mathrm{K}(k)$ is the complete elliptic integral of the second kind. These equations give a complete solution to the problem at leading order and equation (4.66) on its own gives a relationship between the applied voltage and the maximum distortion of the director.

5 Discussion and future work

We have used the Leslie–Ericksen equations to model the static properties of a simple liquid crystal device consisting of a nematic material between two parallel plates whose texture is distorted by the application of an electric field. This serves as an archetype for more complex but realistic liquid crystal devices of practical importance. A systematic asymptotic analysis has been applied and solution derived for the practical range of three nondimensional parameters describing the liquid crystal properties. In particular we have included the interaction between the electric field and the nematic distortion in the model. The solutions give new insight into the behaviour of practical devices where such effects are important. Of particular interest are the solutions (4.26) and (4.27) derived for liquid crystals with low anisotropies subjected to a high applied field. As pointed out these solutions are very robust and are applicable to a wide range of liquid crystal materials of practical interest.

The analysis presented here demonstrates that there is significant benefit to industry to be gained from application of similar methods to models of liquid crystals in more general settings. Although accurate predictions of the liquid crystal distortions and the optical properties of devices can be made using computational methods, the asymptotic methods used in this paper give the device designer a more powerful overview of the type of behaviour that can occur as parameters are changed. There has been some work done in this area, nevertheless there remains a rich vein of analysis to be explored from Leslie-Ericksen theory applied to practical devices. In this paper we have considered a very simple geometry and static solutions. Extensions to twisted nematics and weak anchoring have been considered and will be presented elsewhere. However, extensions to consider the bifurcation properties, the dynamical switching, and more complex geometries remain relatively open questions.

References

[1] Allender, D. W., Crawford, G. P. & Doane, J. W. (1991) Determination of the liquid-crystal surface elastic-constant k_{24}. *Phys. Rev. Lett.* **67**, 1442–1445.

[2] Barbero, G., Miraldi, E., Oldano, C. & Taverna-Valabrega, P. (1988) Freedericksz transition in crossed electric and magnetic fields. *Z. Naturforsch*, **43a**, 547–554.

[3] Barratt, P. J. & Fraser, C. (1983) Some bifurcation problems in cholesteric liquid crystal theory. *Proc. Edin. Math. Soc.* **26**, 319–332.

[4] Berreman, D. W. (1983) Numerical models of twisted nematic devices. *Phil. Trans. Roy. Soc.* **309**, 203–216.

[5] Bouteiller, L. & Le Barny, P. (1996) Polymer-dispersed liquid crystals: Preparation, operation and application. *Liquid Crystals*, **21**, 157–174.
[6] de Gennes, P. G. & Prost, J. (1993) *The Physics of Liquid Crystals*. (2nd edn). Clarendon Press.
[7] Deuling, H. J. (1972) Deformation of nematic liquid crystals in an electric field. *Mol. Cryst. Liq.Cryst*. **19**, 123–131.
[8] Deuling, H. J., Guyon, E. & Pieranski, P. (1974) Deformation of nematic layers in crossed electric and magnetic fields. *Solid State Comm.* **15**, 277–279.
[9] Ericksen, J. L. (1961) Conservation laws for Liquid Crystals. *Trans. Soc. Rheol*. **5**, 23–34.
[10] Ericksen, J. L. (1976) Equilibrium theory of liquid crystals. *Advances in Liquid Crystals*, **2**, 233–298.
[11] Frank, F. C. (1958) On the theory of liquid crystals. *Discuss. Faraday Soc*. **25**, 19–28.
[12] Hinch, E. J. (1991) *Perturbation Methods*. Cambridge University Press.
[13] Klaus, W., Suzuki, Y., Tsuchiya, M. & Kamiya, T. (1995) Optical characterization of homogeneous nematic liquid crystal cells based on the liquid crystal continuum model. *Jpn. J. App. Phys. I* **34**, 6114–6124.
[14] Kramer, L. (ed.) (1996) Pattern Formation in Liquid Crystals. Springer-Verlag.
[15] Lam, L. & Prost, J. (eds.) (1991) Solitons in Liquid Crystals. Springer-Verlag.
[16] Leslie, F. M. (1968) Some constitutive equations for Liquid Crystals. *Arch. Rat. Mech. Anal.* **28**, 265–283.
[17] Leslie, F. M. (1979) Theory of flow phenomena in Liquid Crystals. *Advances in Liquid Crystals*, **4**, 1–81.
[18] Leslie, F. M. (1992) Continuum theory for Nematic Liquid crystals. *Continuum Mech. Thermodyn.* **4**, 167–175.
[19] Leslie, F. M. & Stewart, I. W. (1985) Mathematical models of liquid crystals. *Euro. J. Appl. Math.* **8**, 251–252.
[20] Lien, S. C. A. (1993) Application of computer simulation to improve the optical performance of liquid crystal displays. *Opt. Eng.* **32**, 1762–1768.
[21] Logan, J. D. (1988) *Applied Mathematics, A Contemporary Approach*. Wiley-Interscience.
[22] Lonberg, F. & Meyer, R. B. (1985) New ground state for the splay-Freedericksz transition in a polymer nematic liquid crystal. *Phys. Rev. Lett*. **55**, 718–721.
[23] Parodi, O. (1970) Stress tensor for nematic liquid crystals. *J. Phys. (Paris)*, **31**, 581–584.
[24] Pieranski, P. & Guyon, E. (1973) Shear flow induced transitions in nematics. *Solid State Comm.* **13**, 435–437.
[25] Preist, T. W., Welford, K. R. & Sambles, J. R. (1989) Response of a twisted nematics liquid crystal to any applied potential. *Liquid Crystals*, **4**, 103–116.
[26] Schiller, P. (1989) Perturbation theory for planar nematic twisted layers. *Liquid Crystals*, **4**, 69–78.
[27] Self, R. H. 1998 *Ph.D. Thesis* University of Southampton, UK. (Unpublished.)
[28] Self, R. H., Please, C. P. & Sluckin, T. J. (1999) Travelling-wave relaxation in elongated liquid crystal cells. *Phys. Rev. E*, **60**, 5029–5032.
[29] Sonnet, A. M., Virga, E. G. & Durand, G. E. (2000) Dilution of nematics surface potentials: Relaxation dynamics. *Phys. Rev. E* **62**, 3694–3701.
[30] Stelzer, J., Hirning, R. & Trebin, H.-R. (1993) Influence of surface anchoring and viscosity upon the switching behavior of twisted nematic cells. *J. Appl. Phys.* **74**, 6046–6052.
[31] Virga, E. G. (1994) *Variational Theories for Liquid Crystals*. Chapman & Hall.
[32] Yokoyama, H. (1988) Surface anchoring of nematic liquid crystals. *Mol. Cryst. Liq. Cryst*. **165**, 265–316.